Oxidation behaviors of Ni-base Superalloys for Nuclear Hydrogen production in Steam with and without Hydrogen Environments

Donghoon Kim[a], Jahyun Koo[a], Daejong Kim[b], Young-Sung Yoo[c], and Changheui Jang[a*]
[a]*Dept. of Nuclear and Quantum Engineering, KAIST, Daejeon, KOREA*
[b]*Korea Atomic Energy Research Institute, Daejeon, KOREA*
[c]*Korea Electric Power Research Institute, Daejeon, KOREA*
[*]*Corresponding author: chjang@kaist.ac.kr*

1. Introduction

The high temperature steam electrolysis (HTSE) is one of the promising ways of the massive hydrogen production using the very high temperature gas cooled reactor (VHTR) because they has a higher efficiency below the 850°C and available to adapt the existing solid oxide fuel cell (SOFC) technologies. Intermediate heat exchanger (IHX) is important structural component which supply high temperature steam to the HTSE. Also, steam provided to the HTSE would be mixed with hydrogen in order to ensure reduction environment. Therefore, the candidate IHX materials require the high temperature oxidation resistance in steam with and without hydrogen environments [1].

One of the candidate materials for the IHX is Ni-base superalloys such as Alloy 617 and Haynes 230 due to excellent high temperature oxidation resistance. In this study, oxidation behaviors of Ni-base superalloys were evaluated in steam with and without hydrogen environments.

2. Experimental

Commercial wrought Ni-base superalloys such as Alloy 617 and Haynes 230 were used in this study. The chemical composition of Alloy 617 and Haynes 230 were listed in Table 1. Coupon type specimen with 13mm in diameter and 1mm thickness were used for isothermal oxidation test. Isothermal oxidation test were performed in pure steam and steam + 20vol.%H_2 mixture condition at 900°C up to 1000 hours. The flow rate of steam and steam + 20vol.%H_2 mixture were 20cc/min at room temperature.

Table I: Chemical compositions of Alloy 617 and Haynes 230 (wt.%)

	Ni	Cr	Co	Mo	W	Fe	Al	Mn	Si	Ti	C
Alloy 617	Bal.	21.6	11.8	8.92	-	1.14	1.50	0.05	0.50	0.35	0.10
Haynes 230	Bal.	21.5	0.36	1.06	13.8	2.94	0.29	0.46	0.38	-	0.10

3. Results and discussion

2.1 Oxidation rate

Fig. 1 shows the weight gain curve versus time of Alloy 617 and Haynes 230 in steam and steam + 20vol.%H_2 conditions at 900°C up to 1000hours. Weight gain curves were governed by parabolic rate law in all conditions with distinctive rate change for Haynes 230 after 100 hours. Oxidation rate of Alloy 617 was faster than Haynes 230 in all conditions. For both alloys, oxidation rate was similar in air and steam conditions. On the other hands, hydrogen addition to steam significantly accelerates the oxidation rate for both alloys. In the oxide lattice, hydrogen is easily ionized to protons and affects the defect structure of oxide [2]. If hydrogen were sufficiently ionized to proton, equilibrium chare balance were changed below equations 1

$$3\left[Cr_i^{\cdots}\right]=\left[e'\right]+\left[H_i'\right] \quad (1)$$

Amount of chromium interstitial defects is increased with proton. Consequently, oxidation rates are increase by ionized protons.

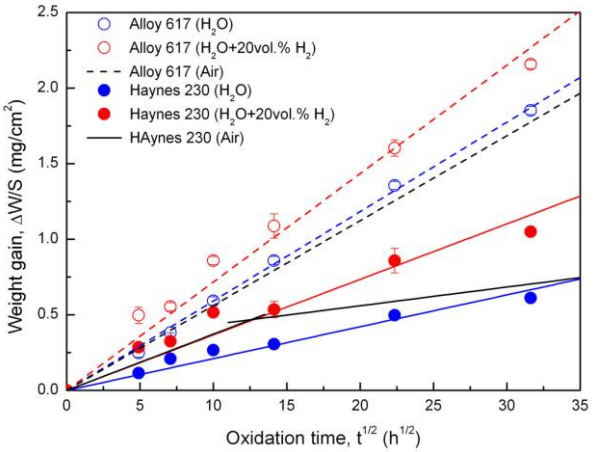

Fig. 1. Weight gain curves of Alloy 617 and Haynes 230 at 900°C in steam with and without hydrogen conditions.

2.2 Microstructure of oxide layer

As previous reported [3] oxide structure of Alloy 617 oxidized in air consist of $NiO/NiCr_2O_4/Cr_2O_3$ external oxide and Al_2O_3 internal oxide along grain boundaries. However, as shown in Fig. 2, outer oxides consist of granular $MnTiO_3$ and Cr_2O_3 layer and sub-layer Cr_2O_3

and internal Al_2O_3 were formed in steam and steam + 20 vol.% H_2 conditions. The equilibrium oxygen partial pressure of NiO is 7×10^{-13}atm at 900°C and that of steam and steam + 20vol.% H_2 is 6.3×10^{-17}atm and 8.47×10^{-16}atm, respectively. Therefore, NiO is no longer stable phase in steam and steam + 20vol.% H_2. Also, diffusion coefficient of Mn and Ti is higher than Ni and Cr in Cr_2O_3 [4] and Ti solubility in Cr_2O_3 was increased with decreasing oxygen partial pressure [5]. Thus, Ti and Mn outward diffusion in Cr_2O_3 were enhanced in steam and steam + 20vol.% H2. Consequently, outmost $MnTiO_3$ was formed. As shown in fig. 3, oxide layer were composed of external $MnCr_2O_4$ and Cr_2O_3 and sub-layer Cr_2O_3 were formed for Haynes 230. In contrast to Alloy 617, outmost $MnCr_2O_4$ oxide layer were formed because of higher Mn contents in Haynes 230 and that effectively suppressed the oxidant ion such as metal cation and oxygen anion diffusion. For both alloys, sub-layer Cr_2O_3 was formed because inward diffusion of oxygen anion was occurred in addition to outward diffusion of metal cation in low oxygen partial pressure such as steam and steam + 20vol.% H_2 environments [6]. Decarburization depth was increased when hydrogen were added. Carbide dissolution was occurred by H_2O penetration through oxide layer.

$$6H_2O + Cr_{23}C_6 \rightarrow 6Co + 23Cr + 6H_2 \quad (2)$$

When hydrogen was added, that easily penetrate to oxide layer and then dissolve the Cr_2O_3.

$$2Cr_2O_3 + 6H_2 \rightarrow 6H_2O + 4Cr \quad (3)$$

Consequently, more H_2O existed at scale and metal interface. Consequently, carbide dissolution was enhanced by equations (2).

3. Conclusions

The oxidation behaviors of Alloy 617 and Haynes 230 in steam and steam + 20vol.% H_2 at 900° were investigated.

Oxide layer of Alloy 617 consist of external $MnTiO_3/Cr_2O_3$, sub-layer Cr_2O_3, and internal Al_2O_3. On the other hands, external $MnCr_2O_4/Cr_2O_3$ double layer were formed.

Low oxygen partial pressure conditions, steam and steam + 20 vol% H_2, change the oxide structures compared air. Ni-rich oxides which were formed in air were not formed and Mn, Ti rich oxides formation were enhanced. Sub-layer Cr_2O_3 were formed by oxygen inward diffusion.

When hydrogen was added in steam condition, oxidation rate was increased because of accelerated outward diffusion of metal cation. Also, carbide dissolution was enhanced due to the added hydrogen.

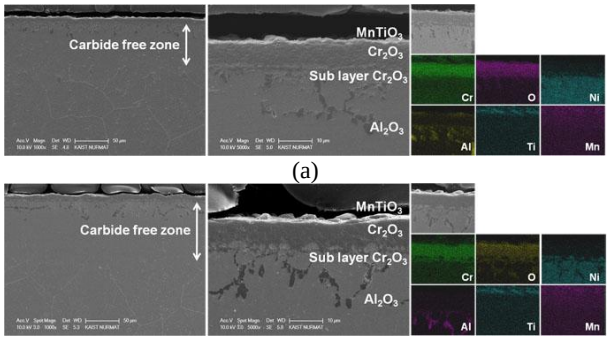

Fig. 2. Oxide layer structure of Alloy 617 oxidized for 1000hours at 900°C in (a) H_2O and (b) H_2O + 20vol.% H_2 conditions.

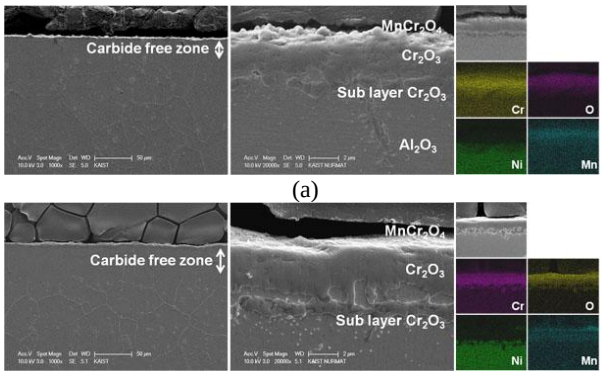

Fig. 3. Oxide layer structure of Haynes 230 oxidized for 1000hours at 900°C in (a) H_2O and (b) H_2O + 20vol.% H_2 conditions.

REFERENCES

[1] A. Brisse, J. Schefold, and M. Zahid, High Temperature Water Electrolysis in Solid Oxide Fuel Cells, International Journal of Hydrogen Energy Vol.33, p.5375, 2008.
[2] T. Norby, Proton Conduction in Oxides, Solid State Ionics Vol.40/41, p.857, 1990.
[3] D. Kim, C. Jang, and W. S. Ryu, Oxidation Characteristics and Oxide Layer Evolution of Alloy 617 and Haynes 230 at 900°C and 1100°C, Oxidation of Metals Vol.71, p.271, 2009.
[4] R.E. Lobnig, H.P. Schmidt, K. Hennesen, and H.J. Grabke, Diffusion of Cations in Chromia Layers Grown on Iron-Base Alloys, Oxidation of Metals, Vol.37, p.81, 1992.
[5] A. Naoumidis, H. A. Schulze, W. Jungen, P. Lersch, Phase Studies in the Chromium-Manganese-Titanium Oxide System at Different Oxygen Partial Pressures, Journal of European Ceramic Society, Vol.**7**, p.55, 1991.
[6] J. Zurek, D.J. Young, E. Essuman, M. Hansel, H.J Penkalla, L. Niewolak, and W.J Quadakkers, Growth and Adherence of Chromia Based Surface Scales on Ni-base Alloys in High- and Low-pO_2 Gases, Materials Science and Engineering A, Vol.477, p.259, 2008.